On the Synthesis of Very Sharp Decimators and Interpolators Using the Frequency-Response Masking Technique

Yong Ching Lim, *Fellow, IEEE,* and Rui Yang

***Abstract*—Decimation and interpolation are very common multirate signal processing operations. Conventional decimation or interpolation technique using polyphase filters has the advantage that for a given transition-band sharpness, the filter's computational complexity decreases with increasing interpolation or decimation factor. Nevertheless, if the transition band of the decimation or interpolation filter is very sharp, the complexity of the filter may still be very high. The complexity of a very sharp filter may be reduced using the frequency-response masking (FRM) technique. However, as shown in this paper, for a given transition-band sharpness, the computational complexity of the classical FRM method does not reduce as rapidly as the increase in decimation or interpolation factor. In this paper, we present a novel variant of the FRM technique for interpolation or decimation application. In this new variant, the computational complexity reduces as rapidly as the interpolation or decimation factor increases. The reduction in computational complexity increases with decreasing transition width. Over an order of magnitude reduction in computational complexity is achieved when compared with conventional polyphase approach in a particular example presented in this paper.**

***Index Terms*—Decimators, FIR filters, frequency-response masking, interpolators, multirate filters, very sharp filters.**

I. Introduction

ALIASING problems arise when the sampling rate of a signal is altered as a result of decimation or interpolation. In order to reduce the aliasing problem to an acceptable level, an anti-aliasing filter is used to filter the signal before decimation or after interpolation. The design of anti-aliasing filters (decimators and interpolators) are well reported in the literature [1]–[5]. In cases where as much of the information must be faithfully preserved as possible, the anti-aliasing filter must have very narrow transition width. The complexity of a finite impulse response (FIR) filter is inversely proportional to its transition width; therefore, filters with very sharp transition widths are very complex. The frequency-response masking (FRM) [6]–[31] technique has been used very successfully in the synthesis of very sharp filters with very low complexity.

In an interpolation process, the input signal's sampling rate is lower than the output signal's sampling rate by a "factor of L," where L is an integer. The input signal is first interpolated by inserting zero and then filtered by the interpolation filter. Since only one out of every L of the input data to the interpolation filter is nonzero, the computational rate of the interpolation filter may be reduced by ignoring all multiplications involving zero value elements. In a decimation process, the input signal is filtered by a decimation filter and only one out of every L samples of the filtered signal is required, where L is the decimation factor; the other outputs are discarded. The computational rate of the decimation filter may also be reduced by ignoring all the discarded outputs. By discarding the multiplications involving zero valued input samples and unwanted output samples, the computational complexity can be reduced by a factor of L; this is referred to as the "factor of L" reduction in computational complexity in this paper. The polyphase technique can easily exploit this "factor of L" reduction in computational rate.

The polyphase technique can be easily applied if the filter is a direct-form FIR filter. If the filter consists of a cascade of two filters, in general, only one of the subfilters may achieve the "factor of L" reduction in computational rate.

A filter synthesized using the FRM technique is essentially a system consisting of FIR subfilters connected in parallel and in cascade. Its z-transform transfer function $H(z)$ is given by

$$H(z) = H_a(z^M)H_{Ma}(z) + (1 - H_a(z^M))H_{Mc}(z). \quad (1)$$

In this paper, we will assume that all the subfilters are zero-phase filters in order to simplify notations. Causality can be easily restored by inserting the appropriate number of delays into the subfilters.

In (1), $H(z)$ and $H_a(z^M)$ are the z-transform transfer functions of the overall filter system and the bandedge-shaping filter, respectively. $H_{Ma}(z)$ and $H_{Mc}(z)$ are the z-transform transfer functions of the masking filters. The bandedge-shaping filter $H_a(z^M)$ is derived from a lowpass prototype filter $H_a(z)$ by substituting one delay element by M delay elements. The complete structure synthesizing (1) is shown in Fig. 1.

The main advantages of the FRM technique are 1) that it employs subfilters with either very short length (in the case of the masking filters) or very sparse coefficient values (in the case of the bandedge-shaping filter) and 2) that the resulting effective

Manuscript received May 24, 2003; revised February 17, 2004. This work was supported in part by Nanyang Technological University, Temasek Laboratories at Nanyang Technological University, and National University of Singapore. The associate editor coordinating the review of this manuscript and approving it for publication was Dr. Anamitra Makur.

Y. C. Lim is with the School of Electrical and Electronics Engineering, Nanyang Technological University, Singapore 639798 (e-mail: elelimyc@pmail.ntu.edu.sg).

R. Yang is with the Agilent Technology Inc., Milpitas, CA 95035 USA (e-mail: anne_yang@agilent.com).

Digital Object Identifier 10.1109/TSP.2005.843743

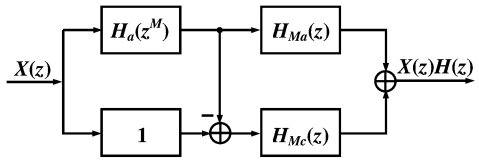

Fig. 1. Structure of a filter synthesized using the FRM technique. All the subfilters are assumed to be zero phase. Causality can be restored by introducing appropriate delays into the subfilters.

filter length is only slightly longer than that of the theoretical (Remez) minimum.

Because of the cascade nature, in general, filters synthesized using the conventional FRM technique cannot benefit fully from the "factor of L" computational advantage of multirate implementation. In this paper, we introduce a variation of the FRM structure. In this variation, the filter system is recast into one consisting of three subfilters. We also show that this variation will benefit fully from the "factor of L" computational complexity reduction of a multirate implementation.

In Section II of this paper, two types of transition-band characteristics for an interpolator or a decimator are presented. The two types of transition-band characteristics give rise to two separate problems in the design of FRM-based interpolation or decimation filter as discussed in Section III. Our new variant of the FRM structure for implementing interpolation and decimation filters is introduced in Sections IV–VI. Polyphase implementation for the new FRM structure is presented in Section VII. In the FRM technique, each delay of the bandedge-shaping filter is replaced by M delays. The optimum value of M for multirate implementation is derived in Section VIII. The effect of the frequency responses of the subfilters on the overall filter's frequency response is discussed in Section IX. In Section X, a very sharp "factor of five" interpolator/decimator example that is designed using our new variant of the FRM structure is presented; over an order of magnitude saving in computational complexity is achieved. The narrowband special case where L is even is presented in Section XI.

II. Transition-Band Characteristics of Interpolation/Decimation Filter

The relationship between the signal frequency spectrum and filter frequency response of an interpolator and a decimator are shown in Fig. 2. For the 1-to-L interpolator, the input signal $x(n)$ is expanded by a factor of L in sampling rate to produce the signal $w(m)$.

The spectrum of $w(m)$ contains not only the baseband spectrum of $x(n)$ but also periodic repetitions (images) of this spectrum, as shown in Fig. 2(c). The lowpass filter $h(m)$ serves as an anti-imaging filter to attenuate these images to produce the output signal $y(m)$. The ideal frequency response of the lowpass filter is

$$\hat{H}(e^{j\omega}) = \begin{cases} 1, & |\omega'| \le \dfrac{\pi}{\mathrm{L}} \\ 0, & \text{otherwise} \end{cases} \tag{2}$$

as illustrated in Fig. 2(d).

The frequency response plots for the various components for an L-to-1 decimator are shown in Fig. 2(g)–(j).

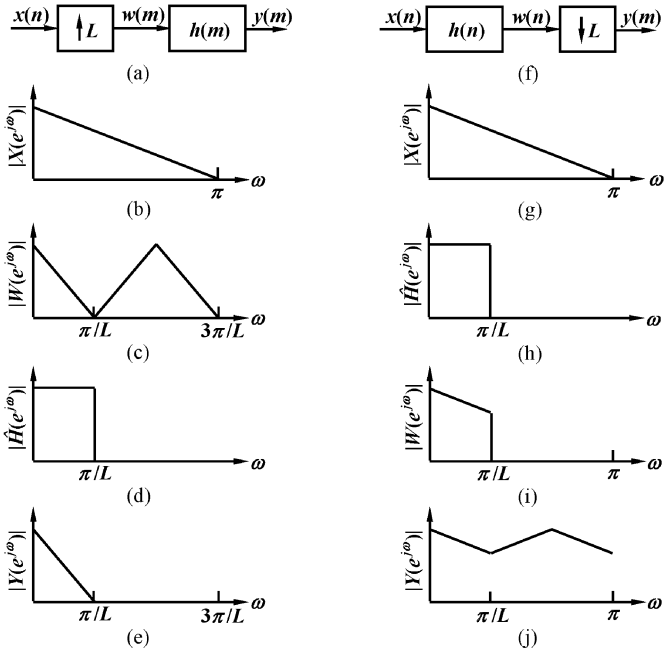

Fig. 2. Frequency spectrum of an Lth interpolation and an Lth decimation process.

In actual implementation, a sharp cut-off filter instead of an ideal filter is used for the interpolator/decimator. Two types of transition band characteristics are shown in Fig. 3. Note that in Fig. 3(a), the stopband edge ω_s is less than or equal to π/L. This type of transition band characteristics places all aliasing energy in the stopband of the filter. Another type where a small amount of the aliasing energy is placed in the transition band of the filter is shown in Fig. 3(b). In this case, ω_s and ω_p are often selected such that $\omega_s - \pi/L = \pi/L - \omega_p$. Since the transition width of the filter used in Fig. 3(b) is twice that in Fig. 3(a), the complexity of the filter in Fig. 3(b) is approximately half that in Fig. 3(a). The transition band of the filters discussed in this paper includes π/L.

III. Problem of the FRM-Based Interpolator/Decimator

The principle of the FRM technique is illustrated in Fig. 1, [6]. We will use the implementation of an interpolator or anti-imaging filter to illustrate the problem encountered by an FRM-based filter. A similar problem arises in the implementation of a decimator. In Fig. 1, $H_a(z^M)$ can be implemented very efficiently using a polyphase structure since the input signals are nonzero only at intervals of L samples. The coefficient values of $H_a(z^M)$ are nonzero at intervals of M samples. The output signal of $H_a(z^M)$ is nonzero at intervals of HCF(M, L), where HCF(M, L) is the highest common factor of M, and L. $H_{Ma}(z)$ and $H_{Mc}(z)$ can be implemented very efficiently using the polyphase structure provided that the output of $H_a(z^M)$ is nonzero at intervals of L samples. Hence, under this condition

$$\mathrm{HCF}(M, L) = L \tag{3}$$

i.e., M is an integer multiple of L. It has been shown in [6] that not all values of M will produce a feasible design. Specifically,

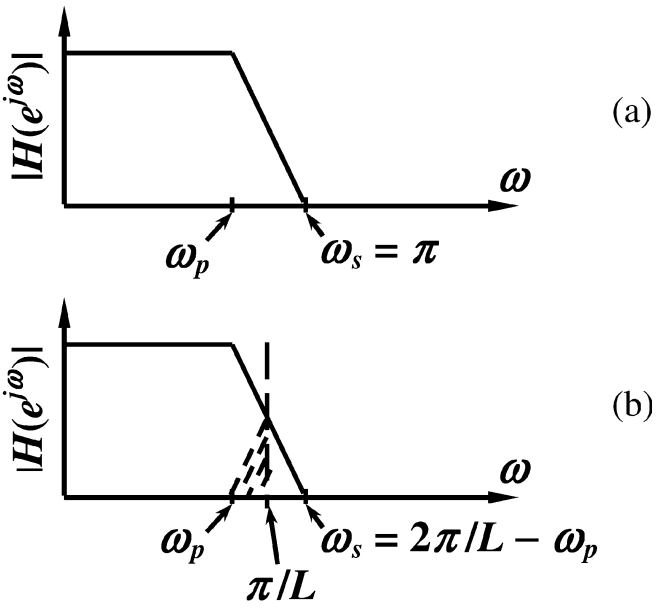

Fig. 3. Frequency responses of interpolator or decimator. (a) Stopband edge $\omega_s = \pi/L$. (b) Stopband edge $\omega_s = 2\pi/L - \omega_p$. The sampling frequency is 2π. L is the interpolation or decimation factor.

the FRM technique will produce a feasible design only if both of the following conditions are satisfied:

Condition 1: Neither $M\omega_p/\pi$ nor $M\omega_s/\pi$ is an integer; ω_p and ω_s are the passband and stopband edges, respectively, and the output sampling frequency is 2π.

Condition 2: $\lfloor M\omega_p/\pi \rfloor = \lfloor M\omega_s/\pi \rfloor$, where $\lfloor x \rfloor$ is the largest integer less than x.

Although it is always possible to find a value of M that will lead to an efficient implementation in the single rate case, it is not so in the multirate case if a factor of L saving in computation load is desired. If the transition band of the filter is centered at π/L so that $\omega_p < \pi/L$ and $\omega_s > \pi/L$, as shown in Fig. 3(b), $M\omega_p/\pi$ will be less than M/L and $M\omega_s/\pi$ will be larger than M/L; if M/L is an integer [as required by (3)], then $\lfloor M\omega_p/\pi \rfloor \neq \lfloor M\omega_s/\pi \rfloor$, and hence, Condition 2 above is violated. If $\omega_s = \pi/L$, as shown in Fig. 3(a), then Condition 1 is violated. Thus, the conventional FRM technique will not be able to benefit fully from the "factor of L" computational saving available from a multirate system.

IV. New Variant of the FRM Structure for Interpolation/Decimation

Reorganizing (1), we have

$$H(z) = H_a(z^M)(H_{Ma}(z) - H_{Mc}(z)) + H_{Mc}(z). \tag{4}$$

Define

$$H_d(z) = H_{Ma}(z) - H_{Mc}(z). \tag{5}$$

From (4) and (5), we have

$$H(z) = H_a(z^M)H_d(z) + H_{Mc}(z) \tag{6}$$

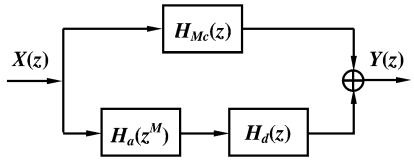

Fig. 4. Alternative realization structure for filters synthesized using the frequency-response-masking technique.

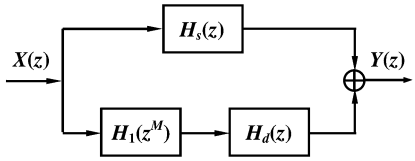

Fig. 5. Variant of the FRM structure suitable for multirate implemention.

giving rise to an alternative realization structure as shown in Fig. 4.

A special case of the variant is when the bandedge-shaping filter $H_a(z^M)$ is derived from a halfband prototype filter. In this special case, the band-edge shaping filter can thus be expressed as

$$H_a(z^M) = 1/2 + H_1(z^M) \tag{7}$$

where

$$H_1(z^M) = \sum_{n=1}^{\frac{N_{ha}+1}{4}} h_a(2n-1)\left(z^{(2n-1)M} + z^{-(2n-1)M}\right) \tag{8}$$

and N_{ha} is the length of $H_a(z)$. Note that $H_1(z^M)$ is a function of z^{-2M}. Substituting (5) and (7) into (6), we have

$$H(z) = H_s(z) + H_1(z^M)H_d(z) \tag{9}$$

where $H_s(z)$ is given by

$$H_s(z) = 1/2(H_{Ma}(z) + H_{Mc}(z)). \tag{10}$$

This gives rise to another variation of the FRM structure shown in Fig. 5. The impulse response of $H_1(z^M)$ is nonzero at an interval of $2M$. $H_s(z)$ and $H_d(z)$ are linear combinations of the masking filters of the conventional FRM technique. This will not introduce extra computational complexity when the lengths of $H_{Ma}(z)$ and $H_{Mc}(z)$ are equal. The structure of Fig. 5 is adopted in our approach. Since $H_a(z)$ is a halfband filter, the transition band characteristics of our approach belongs to the type shown in Fig. 3(b).

The new FRM structure shown in Fig. 5 contains two branches, namely, a) $H_s(z)$ and b) a cascade of $H_1(z^M)$ and $H_d(z)$. For an interpolation process, $H_s(z)$ and $H_1(z^M)$ can be implemented very efficiently using the polyphase structure since their input signals are nonzero only at intervals of L samples. The coefficient values of $H_1(z^M)$ are nonzero at intervals of $2M$ samples. The output signal of $H_1(z^M)$ is nonzero at intervals of HCF$(2M, L)$. $H_d(z)$ can be implemented very efficiently using the polyphase structure, provided that the

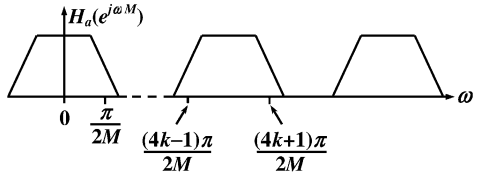

Fig. 6. Frequency response of $H_a(e^{j\omega M})$.

output of $H_1(z^M)$ is nonzero at intervals of L samples. Hence, under this condition

$$\text{HCF}(2M, L) = L. \tag{11}$$

This requires $2M$ to be an integer multiple of L.

V. Even Factor Interpolation/Decimaton

If L is even, it is easy to find a value of M that satisfies (11) as well as Conditions 1 and 2 stated in Section III. We will devote this section to the discussion on the special case where L is even.

As can be seen from Fig. 6, the bandedges of $H_a(e^{j\omega M})$ are centred at $(2k+1)\pi/(2M)$ where k is an integer. (Note that $(4k-1)\pi/(2M)$ and $(4k+1)\pi/(2M)$ may be written collectively as $(2k+1)\pi/(2M)$.) For an interpolation or decimation factor of L, the interpolator's or decimator's bandedge should be centred at π/L. Thus, we have, $(2k+1)\pi/(2M) = \pi/L$ or

$$M = \frac{(2 \times \text{integer} + 1)L}{2} \quad (\text{for } L \text{ even}). \tag{12}$$

Thus, for L even, $2M$ is an odd multiple of L.

VI. Odd Factor Interpolation/Decimation

If L is odd, in order to satisfy (11), M must be an integer multiple of L. If M is an integer multiple of L, Condition 2 will be violated, as already discussed in Section III. This difficulty can be alleviated as follows.

Replacing z by $ze^{-j\pi/(2M)}$ in (7), $H_a(z^M)$ becomes $H_{aI}(z^M)$.

$$\begin{aligned} H_{aI}(z^M) &= \frac{1}{2} + \sum_{n=1}^{\frac{N_{ha}+1}{4}} jh_a(2n-1)\sin\left(n\pi - \frac{\pi}{2}\right) \\ &\quad \times \left(z^{-(2n-1)M} - z^{(2n-1)M}\right) \\ &= \frac{1}{2} + \sum_{n=1}^{\frac{N_{ha}+1}{4}} j(-1)^{n-1}h_a(2n-1) \\ &\quad \times \left(z^{-(2n-1)M} - z^{(2n-1)M}\right). \end{aligned} \tag{13}$$

In this case, $H_1(z^M)$ becomes a complex filter whose coefficient values are purely imaginary.

$$\begin{aligned} H_1(z^M) = \sum_{n=1}^{\frac{N_{ha}+1}{4}} & j(-1)^{n-1}h_a(2n-1) \\ & \times \left(z^{-(2n-1)M} - z^{(2n-1)M}\right). \end{aligned} \tag{14}$$

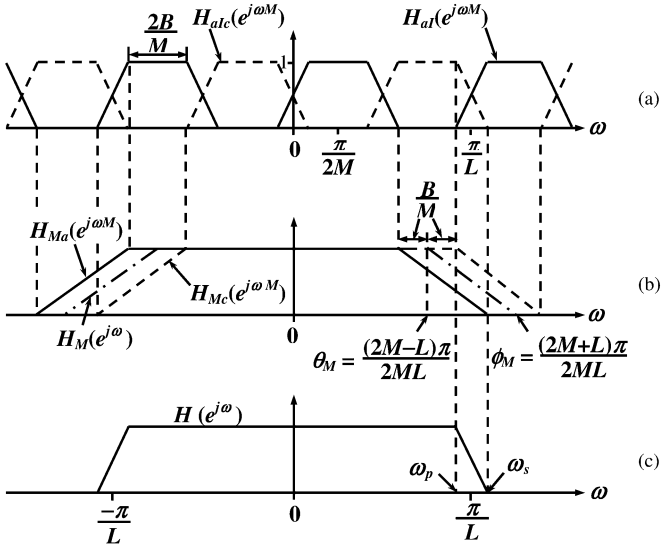

Fig. 7. Frequency responses of the subfilters for odd factor interpolation/decimation. (a) Frequency-response of the bandedge-shaping filter $H_{aI}(z^M)$ and that of its complement. (b) Frequency-responses of the filters $H_{Ma}(z)$, $H_{Mc}(z)$, and $H_M(z)$. (c) Frequency response of the overall filter.

The frequency response of $H_{aI}(z^M)$, which is denoted by $H_{aI}(e^{j\omega M})$, is that of $H_a(z^M)$ shifted to the right by $\pi/(2M)$, as shown by the solid-line plot in Fig. 7(a). Let $H_{aIc}(z^M)$ be the complementary filter of $H_{aI}(z^M)$. Thus

$$\begin{aligned} H_{aIc}(z^M) &= \frac{1}{2} - \sum_{n=1}^{\frac{N_{ha}+1}{4}} j(-1)^{n-1}h_a(2n-1) \\ &\quad \times \left(z^{-(2n-1)M} - z^{(2n-1)M}\right) \\ &= \frac{1}{2} + \sum_{n=1}^{\frac{N_{ha}+1}{4}} j(-1)^{n}h_a(2n-1) \\ &\quad \times \left(z^{-(2n-1)M} - z^{(2n-1)M}\right). \end{aligned} \tag{15}$$

The frequency response of $H_{aIc}(z^M)$, which is denoted by $H_{aIc}(e^{j\omega M})$, is shown as the dash-line plot in Fig. 7(a). The plot for $H_{aIc}(e^{j\omega M})$ is that for $H_a(e^{j\omega M})$ shifted to the left by $\pi/(2M)$. The plot for $H_{aIc}(e^{j\omega M})$ and that for $H_{aI}(e^{j\omega M})$ are mirror images about $\omega = 0$.

Let the frequency responses of the masking filters $H_{Ma}(z)$ and $H_{Mc}(z)$ be $H_{Ma}(e^{j\omega})$ and $H_{Mc}(e^{j\omega})$, respectively. The plots for $H_{Ma}(e^{j\omega})$ and $H_{Mc}(e^{j\omega})$, where the bandedge of $H(e^{j\omega})$ for $\omega > 0$ is determined by $H_{aIc}(e^{j\omega M})$ and those for $\omega < 0$ is determined by $H_{aI}(e^{j\omega M})$, are shown in Fig. 7(b). (The role for $H_{Ma}(e^{j\omega})$ and $H_{Mc}(e^{j\omega})$ are swapped if $H_{aI}(e^{j\omega M})$ determines the bandedge for $\omega > 0$ and $H_{aIc}(e^{j\omega M})$ determines that for $\omega < 0$.) As can be seen from Fig. 7(b), $H_{Ma}(e^{j\omega})$ and $H_{Mc}(e^{j\omega})$ are mirror images about $\omega = 0$. Both of them can be obtained from a prototype masking filter $H_M(e^{j\omega})$ by shifting its frequency response by B/M to the left and right, respectively, where B [see Fig. 7(a)] is the passband width of the prototype bandedge-shaping filter

$H_a(z)$. Referring to Fig. 7, the bandedges of the prototype masking filter $H_M(z)$ are

$$\text{passband edge: } \theta_M = \frac{(2M-L)\pi}{2ML} \quad \text{and} \tag{16}$$

$$\text{stopband edge: } \phi_M = \frac{(2M+L)\pi}{2ML}. \tag{17}$$

Let the length of $H_M(z)$ be N_{hm}. Let the nth coefficient values of $H_M(z)$ be $h_m(n)$. For N_{hm} odd, $H_M(z)$ may be written as

$$H_M(z) = h_m(0) + \sum_{n=1}^{\frac{N_{hm}+1}{2}} h_m(n)(z^{-n} + z^n). \tag{18a}$$

For N_{hm} even, $H_M(z)$ may be written as

$$H_M(z) = \sum_{n=1}^{\frac{N_{hm}+1}{2}} h_m(n)\left(z^{-(n-0.5)} + z^{n-0.5}\right). \tag{18b}$$

$H_{Ma}(z)$ and $H_{Mc}(z)$ are derived from $H_M(z)$ by replacing z by $ze^{-jB/M}$ and $ze^{jB/M}$, respectively. Thus

$$H_{Ma}(z) = H_M(ze^{-jB/M}) \tag{19}$$

and

$$H_{Mc}(z) = H_M(ze^{jB/M}). \tag{20}$$

It is straightforward to show that the coefficient values of $H_{Ma}(z)$ are the complex conjugate of those of $H_{Mc}(z)$. Thus, for L odd, we have

$$H_s(z) = 1/2(H_{Ma}(z) + H_{Mc}(z)) = \text{Re}\{H_{Ma}(z)\} \tag{21}$$

and

$$H_d(z) = H_{Ma}(z) - H_{Mc}(z) = 2\text{Im}\{H_{Ma}(z)\} \tag{22}$$

where $\text{Re}\{H_{Ma}(\text{z})\}$ is a filter whose coefficient values are the real part of the coefficient values of $H_{Ma}(z)$, and $\text{Im}\{H_{Ma}(z)\}$ is a filter whose coefficient values are the imaginary part of the coefficient values of $H_{Ma}(z)$. Thus, in Fig. 5, $H_1(z^M)$ and $H_d(z)$ are filters with purely imaginary coefficients, whereas $H_s(z)$ is a real coefficient filter. The overall output is real.

For N_{hm} odd, from (18a), (19), and (21), $H_s(z)$ may be written as

$$H_s(z) = h_m(0) + \sum_{n=1}^{\frac{N_{hm}+1}{2}} h_m(n)\cos\left(\frac{Bn}{M}\right)(z^{-n} + z^n). \tag{23a}$$

For N_{hm} even, from (18b), (19), and (21), $H_s(z)$ may be written as

$$H_s(z) = \sum_{n=1}^{\frac{N_{hm}+1}{2}} h_m(n)\cos\left(\frac{B(n-0.5)}{M}\right)(z^{-n} + z^n) \tag{23b}$$

For N_{hm} odd, from (18a), (19), and (22), $H_d(z)$ may be written as

$$H_d(z) = 2j \sum_{n=1}^{\frac{N_{hm}+1}{2}} h_m(n)\sin\left(\frac{Bn}{M}\right)(z^{-n} - z^n). \tag{24a}$$

For N_{hm} even, from (18b), (19), and (22), $H_d(z)$ may be written as

$$H_d(z) = 2j \sum_{n=1}^{\frac{N_{hm}+1}{2}} h_m(n)\sin\left(\frac{B(n-0.5)}{M}\right)(z^{-n} - z^n) \tag{24b}$$

As can be seen in Fig. 7, the bandedges of $H_{aI}(e^{j\omega M})$ or $H_{aIc}(e^{j\omega M})$ centers at $k\pi/M$, where k is an integer. Since the interpolator's or decimator's bandedge should be centered at π/L, we have $k\pi/M = \pi/L$ or

$$M = \text{integer} \times L \,(\text{for } L \text{ odd}) \tag{25}$$

Thus, for L odd, $2M$ is an even multiple of L.

VII. Polyphase Form

Equation (8) may be rewritten as

$$H_1(z^M) = z^{-M}H_2(z^{2M}) \tag{26}$$

where, for L even, $H_2(z^{2M})$ is given by

$$H_2(z^M) = \sum_{n=1}^{\frac{N_{ha}+1}{4}} h_a(2n-1)\left(z^{2nM} + z^{-(2n-2)M}\right) \tag{27a}$$

and, for L odd, $H_2(z^{2M})$ is given by

$$H_2(z^M) = \sum_{n=1}^{\frac{N_{ha}+1}{4}} j(-1)^{n-1}h_a(2n-1) \times \left(z^{2nM} + z^{-(2n-2)M}\right). \tag{27b}$$

Let $H_{s,n}(z^L), n = 0, 1, \ldots, L-1$ be the nth polyphase component of $H_s(z)$. Thus, we have

$$H_s(z) = \sum_{n=1}^{L-1} z^{-n}H_{s,n}(z^L). \tag{28}$$

Let $H_{d,n,k}(z^{2M}), n = 0, 1, \ldots, L-1, k = 0, 1, \ldots, 2M/L-1$ be the (n,k)th polyphase component of $H_d(z)$. Thus, we have

$$H_d(z) = \sum_{k=0}^{\frac{2M}{L}-1} z^{-kL} \sum_{n=0}^{L-1} z^{-n}H_{d,n,k}(z^{2M}). \tag{29}$$

From (9), (26), (28), and (29), $H(z)$ may be rewritten in terms of its polyphase components as

$$H(z) = \sum_{n=0}^{L-1} z^{-n} H_{s,n}(z^L) + z^{-M} H_2(z^{2M}) \times \sum_{k=0}^{\frac{2M}{L}-1} z^{-kL} \sum_{n=0}^{L-1} z^{-n} H_{d,i,k}(z^{2M}). \quad (30)$$

VIII. Optimum M

The optimal (Remez) length N_0 of a lowpass filter with normalized transition width β is given approximately by the expression [32]

$$N_0 \approx \frac{\Phi_1(\delta_p, \delta_s)}{\beta} + \Phi_2(\delta_p, \delta_s)\beta + 1 \quad (31)$$

where δ_p and δ_s are the passband and stopband ripple magnitudes, respectively. Note that $\delta_p = \delta_s$ for a halfband filter. For completeness, expressions for $\Phi_1(\delta_p, \delta_s)$ and $\Phi_2(\delta_p, \delta_s)$ are listed in the Appendix. It can be easily verified by substituting suitable values that for $\beta \leq 0.2$, the first term becomes the dominant term. Thus, we have

$$N_0 \approx \frac{\Phi_1(\delta_p, \delta_s)}{\beta} \quad \text{for } \beta \leq 0.2. \quad (32)$$

Using our new method, the peak ripple magnitude of the bandedge-shaping filter and masking filters should be less than that of the maximum allowed ripple magnitude of the overall filter $H(z)$ because the bandedge-shaping filter $H_1(z^M)$ is cascaded with $H_d(z)$. However, this does not significantly affect the filter length because the filter length is more sensitive to transition width than to ripple magnitude. Moreover, the ripple of $H_1(z^M)$ can partially compensate for the ripple of $H_d(z)$. Details of the compensation effect has been discussed in [6]. Furthermore, we are only interested in estimating a good value for M. Thus, the filter length of the prototype bandedge-shaping filter whose transition width is M times that of the overall filter is approximately N_0/M. Taking into account that the prototype bandedge-shaping filter is a halfband filter where half of the coefficient values are zero, the number of nonzero coefficient values (N_{coeff}) for $H_1(z^M)$ is given by

$$N_{\text{coeff}} \approx \frac{N_0}{2M}. \quad (33)$$

The transition widths of $H_{Ma}(z)$ and $H_{Mc}(z)$ are each $f_s/(2M)$. Applying the result of (32), the length of each of the masking filters is $2M\beta N_0$. This is also the filter lengths of $H_d(z)$ and $H_s(z)$. Thus, the lengths of $H_d(z)$ and $H_s(z)$ denoted by N_d and N_s, respectively, are

$$N_d \approx N_s \approx 2M\beta N_0.$$

The total number of nonzero coefficients, which is denoted by $N_{T\text{coeff}}(M)$, is, therefore, given by

$$N_{T\text{coeff}}(M) \approx \left(\frac{1}{2M} + 4M\beta\right) N_0. \quad (34)$$

Let $M_{\min 1}$ be the value of M that minimizes $N_{T\text{coeff}}(M)$. To find $M_{\min 1}$, differentiate $N_{T\text{coeff}}(M)$ with respect to M and equate the derivative to zero. Thus, we have

$$M_{\min 1} = \frac{1}{2\sqrt{2\beta}}. \quad (35)$$

Substituting (35) into (34), $N_{T\text{coeff}}(M_{\min 1})$ is less than N_0 (the number of coefficients required by the conventional polyphase technique) if β is less than 1/8.

If $M = M_{\min 1}$ satisfies either (12) or (25) (depending on the parity of L), then $M_{\min 1}$ is selected as the value of M. If $M = M_{\min 1}$ satisfies neither (12) nor (25), then the value of M used is one that satisfies either (12) or (25) and is in the vicinity of $M_{\min 1}$. Thus, for L even, we choose

$$M = \left\lfloor \frac{1}{L\sqrt{2\beta}} + 0.5 \right\rfloor \frac{L}{2} \quad (36a)$$

and, for L odd, we choose

$$M = \left\lfloor \frac{1}{2L\sqrt{2\beta}} + 0.5 \right\rfloor L. \quad (36b)$$

In polyphase implementation, full exploitation of the filter coefficient's symmetry to reduce computational complexity often leads to other complications such as requiring an excessive number of delays [33]–[35]. In the FRM technique, for $M \geq L$, it is straightforward to exploit the coefficient symmetry of $H_1(z^M)$ to reduce computational complexity. Nevertheless, just like the conventional polyphase filter, the coefficient symmetry for $H_d(z)$ and $H_s(z)$ cannot be easily exploited without introducing other complications. We will now consider the computational complexity where the coefficient symmetry for $H_1(z^M)$ is exploited, but those for $H_d(z)$ and $H_s(z)$ are not. Let N_{mul} be the number of multipliers for $H_1(z^M)$ after considering coefficient symmetry.

$$N_{\text{mul}} \approx \frac{N_0}{4M}. \quad (37)$$

The number of multipliers for $H_d(z)$ and $H_s(z)$ are the same as their filter length since their coefficient symmetry are not exploited. Thus, the total number of multipliers, which is denoted by $N_{T\text{mul}}(M)$, required for $M \geq L$ is given by

$$N_{T\text{mul}}(M) \approx \left(\frac{1}{4M} + 4M\beta\right) N_0. \quad (38)$$

To determine $M_{\min 2}$, the value of M that minimizes $N_{T\text{mul}}(M)$, differentiate $N_{T\text{mul}}(M)$ with respect to M, and equate the derivative to zero. Thus, we have

$$M_{\min 2} = \frac{1}{4\sqrt{\beta}}. \quad (39)$$

Substituting (39) into (38), $N_{T\text{mul}}(M_{\min 2})$ is less than N_0 (the number of multiplications required by the conventional polyphase technique if coefficient symmetry is not exploited) if β is less than 1/4; if $\beta = 1/4$, $M_{\min 2} = 1/2$ and is not an acceptable value since M must be an integer. Substituting $M = 1$ into (38), $N_{T\text{mul}}(M_{\min 2})$ is less than N_0 if β is less than 3/16.

If $M = M_{\min 2}$ satifies neither (12) nor (25), then the value of M used is one that satisfies either (12) or (25) and is in the vicinity of $M_{\min 2}$. Thus, for L even, we choose

$$M = \left\lfloor \frac{1}{2L\sqrt{\beta}} + 0.5 \right\rfloor \frac{L}{2} \tag{40a}$$

and, for L odd, we choose

$$M = \left\lfloor \frac{1}{4L\sqrt{\beta}} + 0.5 \right\rfloor L. \tag{40b}$$

IX. Frequency Responses of $H_s(z), H_d(z)$ and $H_1(z)$

The overall frequency response of the filter is not determined by all the component filters at equal weighting over all frequencies. Knowledge of how the frequency responses of the component filters affect the overall frequency response is important for controlling the convergence of nonlinear optimization algorithms when they are used for the design of the component filters. This section is devoted to the discussion on the relationship between the frequency ripples of the various filters. Let the frequency responses of $H_{Ma}(z), H_{Mc}(z), H_1(z^M), H_s(z), H_d(z)$, and $H(z)$ be $H_{Ma}(e^{j\omega}), H_{Mc}(e^{j\omega}), H_1(e^{jM\omega}), H_s(e^{j\omega}), H_d(e^{j\omega})$, and $H(e^{j\omega})$, respectively. $H_x(e^{j\omega})$ [and, subsequently, $G_x(e^{j\omega})$ and $\delta_x(e^{j\omega})$] are real, where the subscript x represents Ma, Mc, etc. $H_s(z)$ is half the sum of $H_{Ma}(z)$ and $H_{Mc}(z)$. As can be seen from Fig. 8(c), $H_s(e^{j\omega})$ is the frequency response of a lowpass filter with wide transition width. $H_d(e^{j\omega})$, which is shown in Fig. 8(d), masks and shapes $H_1(e^{jM\omega})$, which is shown in Fig. 8(a) to produce the frequency response shown in Fig. 8(e). It is interesting to see that $H_d(e^{j\omega})\ H_1(e^{jM\omega})$ is the correction term needed to sharpen $H_s(e^{j\omega})$ to produce a very sharp $H(e^{j\omega})$. The frequency responses shown in Fig. 8 correspond to those where the transition band of the overall filter is determined by that of $H_1(z)$. A set of similar frequency responses can be drawn for those where the transition band of the overall filter is determined by the complement of $H_1(z)$.

Let the desired values of $H_{Ma}(e^{j\omega}), H_{Mc}(e^{j\omega}), H_1(e^{jM\omega}), H_s(e^{j\omega}), H_d(e^{j\omega})$, and $H(e^{j\omega})$ be $G_{Ma}(e^{j\omega}), G_{Mc}(e^{j\omega}), G_1(e^{jM\omega}), G_s(e^{j\omega}), G_d(e^{j\omega})$, and $G(e^{j\omega})$, respectively. $G_{Ma}(e^{j\omega}), G_{Mc}(e^{j\omega}), G_s(e^{j\omega}), G_d(e^{j\omega})$, and $G(e^{j\omega})$ equal unity in their respective passbands and equal zero in their respective stopbands. $G_1(e^{jM\omega})$ is 0.5 in the passband of $H_a(z^M)$ and is -0.5 in the stopband of $H_a(z^M)$. Let the ripple of $H_{Ma}(e^{j\omega}), H_{Mc}(e^{j\omega}), H_1(e^{jM\omega}), H_s(e^{j\omega}), H_d(e^{j\omega})$, and $H(e^{j\omega})$ be $\delta_{Ma}(e^{j\omega}), \delta_{Mc}(e^{j\omega}), \delta_1(e^{jM\omega}), \delta_s(e^{j\omega}), \delta_d(e^{j\omega})$, and $\delta(e^{j\omega})$, respectively. Thus, we have

$$H_{Ma}(e^{j\omega}) = G_{Ma}(e^{j\omega}) + \delta_{Ma}(e^{j\omega}) \tag{41}$$
$$H_{Mc}(e^{j\omega}) = G_{Mc}(e^{j\omega}) + \delta_{Mc}(e^{j\omega}) \tag{42}$$
$$H_1(e^{jM\omega}) = G_1(e^{jM\omega}) + \delta_1(e^{jM\omega}) \tag{43}$$
$$H_s(e^{j\omega}) = G_s(e^{j\omega}) + \delta_s(e^{j\omega}) \tag{44}$$
$$H_d(e^{j\omega}) = G_d(e^{j\omega}) + \delta_d(e^{j\omega}) \tag{45}$$
$$H(e^{j\omega}) = G(e^{j\omega}) + \delta(e^{j\omega}) \tag{46}$$

We will assume that the frequency response at the transition band of a subfilter is its desired frequency response. Thus, the frequency response ripple of a subfilter at the transition band is zero. We will analyze the frequency response ripple on several frequency ranges.

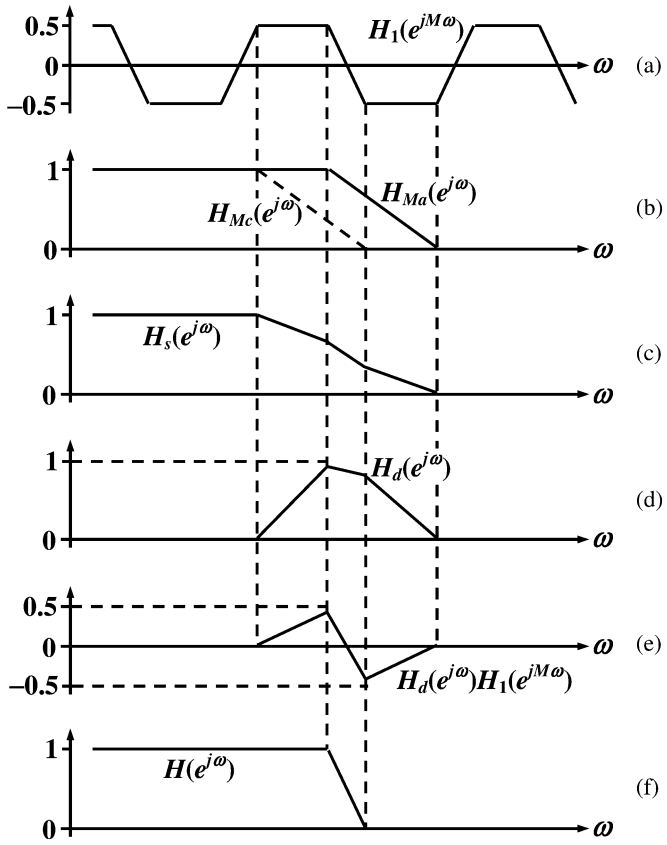

Fig. 8. Frequency responses of (a) $H_1(z^M)$, (b) $H_{ma}(z)$, and $H_{Mc}(z)$, (c) $H_s(z) = 0.5 \times (H_{Ma}(z) + H_{Mc}(z))$, (d) $H_d(z) = H_{Ma}(z) - H_{Mc}(z)$, (e) $H_d(z)H_1(z^M)$, and (f) $H(z) = H_s(z) + H_1(z)H_d(z)$.

Frequency Range I: Within the passband and stopband of $H_s(e^{j\omega})$

From (21), (41), (42), and (44), $\delta_s(e^{j\omega})$ is given by

$$\delta_s(e^{j\omega}) = 0.5 \times (\delta_{Mc}(e^{j\omega}) + \delta_{Ma}(e^{j\omega})). \tag{47}$$

From (22), (41), and (42), $H_d(e^{j\omega})$ is given by

$$H_d(e^{j\omega}) = \delta_d(e^{j\omega}) = \delta_{Ma}(e^{j\omega}) - \delta_{Mc}(e^{j\omega}). \tag{48}$$

Thus, ignoring second-order terms, $H_d(e^{j\omega})H_1(e^{jM\omega})$ is given by

$$H_d(e^{j\omega})H_1(e^{jM\omega}) = 0.5 \times (\delta_{Ma}(e^{j\omega}) - \delta_{Mc}(e^{j\omega})) \text{ for } G_1(e^{jM\omega}) \text{ equals } 0.5 \tag{49a}$$
$$= 0.5 \times (\delta_{Mc}(e^{j\omega}) - \delta_{Ma}(e^{j\omega})) \text{ for } G_1(e^{jM\omega}) \text{ equals } -0.5. \tag{49b}$$

From (9), (44), (47), and (49), ignoring second-order terms, $\delta(e^{j\omega})$ is given by

$$\delta(e^{j\omega}) = (0.5 + G_1(e^{jM\omega})) + \delta_{Ma}(e^{j\omega}) + (0.5 - G_1(e^{jM\omega}))\delta_{Mc}(e^{j\omega}) \tag{50a}$$
$$= \delta_{Ma}(e^{j\omega}) \text{ for } G_1(e^{jM\omega}) \text{ equals } 0.5 \tag{50b}$$
$$= \delta_{Mc}(e^{j\omega}) \text{ for } G_1(e^{jM\omega}) \text{ equals } -0.5. \tag{50c}$$

$H_{Ma}(e^{j\omega})$ and $H_{Mc}(e^{j\omega})$ are derived from $H_M(e^{j\omega})$. It can be seen from Fig. 7 that the frequency range of $H_{Mc}(e^{j\omega})$

for which $G_1(e^{jM\omega})$ equals -0.5 and the frequency rage of $H_{Ma}(e^{j\omega})$ for which $G_1(e^{jM\omega})$ equals 0.5 map to the same frequency range of $H_M(e^{j\omega})$. Thus, if the bandedge of $H(e^{j\omega})$ is determined by that of $H_{aIc}(e^{j\omega M})$ (i.e., if M is an odd multiple of L), the ripples of $H_M(e^{j\omega})$ in the frequency ranges $((2M + L - 4iL)\pi - 2BL)/(2ML)$ to $(2M+L-4iL)\pi/(2ML), i = 1, 2, 3, \ldots, (M-L)/(2L)$ and the frequency ranges $((2M + L + 4Li)\pi - 4BL)/(2ML)$ to $(2M+L+4Li)\pi/(2ML), i = 1, 2, 3, \ldots, M(L-1)/(2L)-1$ contribute only to the second-order term of the ripple of $H(e^{j\omega})$. If the bandedge of $H(e^{j\omega})$ is determined by that of $H_{aI}(e^{j\omega M})$ (i.e., if M is an even multiple of L), the ripples of $H_M(e^{j\omega})$ in the frequency ranges $((2M + 3L)\pi - 4BL - 4\pi Li)/(2ML)$ to $((2M + 3L)\pi - 2\pi L - 4\pi Li)/(2ML), i = 1, 2, 3 \ldots, M/(2L)$ and in the frequency ranges $((2M + L)\pi - 4BL + 4\pi Li)/(2ML)$ to $((2M+L)\pi+4\pi Li)/(2ML), i = 1, 2, 3, \ldots, M(L-1)/(2L)$ contribute only to the second-order term of the ripple of $H(e^{j\omega})$.

Frequency Range II: Within the transition band of $H_s(e^{j\omega})$ and the band where $H_1(e^{j\omega}) = \pm 0.5$.

This corresponds to the frequency ranges from $((2M - L)\pi - 4BL)/(2ML)$ to $(2M - L)\pi/(2ML)$ and from $(2M + L)\pi/(2ML)$ to $(2M + 3L)\ \pi/(2ML)$ for $H_M(e^{j\omega})$. From (9), (21), (22), and (43)–(46), we have

$$\begin{aligned} &G(e^{j\omega}) + \delta(e^{j\omega}) \\ &\quad = G_s(e^{j\omega}) + \delta_s(e^{j\omega}) + (G_1(e^{jM\omega}) \\ &\qquad + \delta_1(e^{jM\omega}))(G_d(e^{j\omega}) + \delta_d(e^{j\omega})) \\ &\quad = 0.5(G_{Ma}(e^{j\omega}) + G_{Mc}(e^{j\omega}) \\ &\qquad + \delta_{Ma}(e^{j\omega}) + \delta_{Mc}(e^{j\omega})) + (G_1(e^{jM\omega}) \\ &\qquad + \delta_1(e^{jM\omega}))(G_d(e^{j\omega}) + \delta_{Ma}(e^{j\omega}) - \delta_{Mc}(e^{j\omega})). \quad (51) \end{aligned}$$

Ignoring second-order terms, we have

$$\begin{aligned} \delta(e^{j\omega}) &= \delta_{Ma}(e^{j\omega}) + G_d(e^{j\omega})\delta_1(e^{jM\omega}) \\ &\qquad \text{for } G_1(e^{jM\omega}) \text{ equals } 0.5 \quad (52a) \\ &= \delta_{Mc}(e^{j\omega}) + G_d(e^{j\omega})\delta_1(e^{jM\omega}) \\ &\qquad \text{for } G_1(e^{jM\omega}) \text{ equals } -0.5. \quad (52b) \end{aligned}$$

Thus, when the magnitude of $G_d(e^{j\omega})$ is small, $\delta(e^{j\omega})$ is determined mainly by either $\delta_{Ma}(e^{j\omega})$ or $\delta_{Mc}(e^{j\omega})$. As $G_d(e^{j\omega})$ approaches unity, the peak value of $|\delta(e^{j\omega})|$ is bounded by $|\delta_{Ma}(e^{j\omega})| + |\delta_1(e^{jM\omega})|$.

X. Example

We arbitrarily choose the design of a "factor of 5" interpolation filter with a transition width of $0.001f_s$, where f_s is the output sampling frequency, as an example to illustrate our method. The transition width is centered at $f_s/10$. The passband and stopband peak ripple magnitude is 0.01. The estimated length [32] of the (Remez) optimum filter meeting this specification is 1945. Thus, the computational rate is $389(=1945/5)$ multiplications per output sample when implemented using the conventional polyphase technique.

For our new method, we have $M_{\min 1} = 11$ (and $M_{\min 2} = 8$). Thus, we choose $M = 10$. The lengths of the bandedge-shaping filter and two masking filters are 195, 43, and 43, respectively. The allowed peak ripple ratios for $H_M(e^{j\omega})$ are tabulated in Table I. The impulse responses for $H_M(z)$ and $H_1(z)$ are tabulated in Tables II and III, respectively. The frequency response of the filter is shown in Fig. 9. As can be seen from the frequency response plots in Fig. 9, the frequency response ripple changes rapidly near the transition edge; this is a typical characteristic of the frequency response of a filter synthesized using the FRM technique. The frequency responses of the subfilters are shown in Fig. 10. As can seen from Fig. 10(b), $H_s(z)$ is a filter with wide transition band. The frequency response of $H_d(z)$ [Fig. 10(c)] masks and shapes that of $H_1(z^{10})$ [Fig. 10(d)] to produce the sharp frequency-response change [Fig. 10(e)]. The frequency response of $H_1(z^{10})\ H_d(z)$ is particularly interesting. Within the passband of $H(z)$, it adds to the frequency response of $H_s(z)$, boosting it to unity. Within the stopband of $H(z)$, it cancels the frequency response of $H_s(z)$, nullifying it to zero. The computational rate is 36.6 [26.8 if symmetry of $H_1(z^M)$ is considered] multiplications per output sample. This corresponds to a saving of over an order of magnitude when compared to the conventional polyphase implementation!

TABLE I
Ratio of Allowed Ripple Peak for $H_M(e^{j\omega})$

Ripple ratio	Frequency range / 2π
3	0.000 – 0.025
1	0.025 – 0.026
0.85	0.026 – 0.075
0.85	0.125 – 0.175
1	0.175 – 0.176
3	0.176 – 0.225
1	0.225 – 0.276
3	0.276 – 0.325
1	0.325 – 0.376
3	0.376 – 0.425
1	0.425 – 0.476
3	0.476 – 0.500

TABLE II
Coefficient Values for $H_M(z)$

$h_M(-21) =$	$0.00639 = h_M(21)$
$h_M(-20) =$	$-0.00201 = h_M(20)$
$h_M(-19) =$	$-0.00470 = h_M(19)$
$h_M(-18) =$	$-0.00682 = h_M(18)$
$h_M(-17) =$	$-0.00760 = h_M(17)$
$h_M(-16) =$	$-0.00564 = h_M(16)$
$h_M(-15) =$	$-0.00032 = h_M(15)$
$h_M(-14) =$	$0.00653 = h_M(14)$
$h_M(-13) =$	$0.01215 = h_M(13)$
$h_M(-12) =$	$0.01515 = h_M(12)$
$h_M(-11) =$	$0.01489 = h_M(11)$
$h_M(-10) =$	$-0.00144 = h_M(10)$
$h_M(-9) =$	$-0.01677 = h_M(9)$
$h_M(-8) =$	$-0.03244 = h_M(8)$
$h_M(-7) =$	$-0.03858 = h_M(7)$
$h_M(-6) =$	$-0.02871 = h_M(6)$
$h_M(-5) =$	$-0.00028 = h_M(5)$
$h_M(-4) =$	$0.04391 = h_M(4)$
$h_M(-3) =$	$0.09667 = h_M(3)$
$h_M(-2) =$	$0.14848 = h_M(2)$
$h_M(-1) =$	$0.18814 = h_M(1)$
$h_M(0) =$	0.19842

TABLE III
COEFFICIENT VALUES FOR $H_1(z)$

$h_1(-97) = -0.00665 = -h_1(97)$	$h_1(-47) = -0.00529 = -h_1(47)$
$h_1(-95) = 0.00060 = -h_1(95)$	$h_1(-45) = -0.00567 = -h_1(45)$
$h_1(-93) = -0.00185 = -h_1(93)$	$h_1(-43) = -0.00606 = -h_1(43)$
$h_1(-91) = -0.00067 = -h_1(91)$	$h_1(-41) = -0.00650 = -h_1(41)$
$h_1(-89) = -0.00149 = -h_1(89)$	$h_1(-39) = -0.00695 = -h_1(39)$
$h_1(-87) = -0.00122 = -h_1(87)$	$h_1(-37) = -0.00748 = -h_1(37)$
$h_1(-85) = -0.00157 = -h_1(85)$	$h_1(-35) = -0.00802 = -h_1(35)$
$h_1(-83) = -0.00154 = -h_1(83)$	$h_1(-33) = -0.00867 = -h_1(33)$
$h_1(-81) = -0.00174 = -h_1(81)$	$h_1(-31) = -0.00935 = -h_1(31)$
$h_1(-79) = -0.00181 = -h_1(79)$	$h_1(-29) = -0.01016 = -h_1(29)$
$h_1(-77) = -0.00198 = -h_1(77)$	$h_1(-27) = -0.01104 = -h_1(27)$
$h_1(-75) = -0.00209 = -h_1(75)$	$h_1(-25) = -0.01209 = -h_1(25)$
$h_1(-73) = -0.00227 = -h_1(73)$	$h_1(-23) = -0.01327 = -h_1(23)$
$h_1(-71) = -0.00241 = -h_1(71)$	$h_1(-21) = -0.01469 = -h_1(21)$
$h_1(-69) = -0.00259 = -h_1(69)$	$h_1(-19) = -0.01638 = -h_1(19)$
$h_1(-67) = -0.00276 = -h_1(67)$	$h_1(-17) = -0.01845 = -h_1(17)$
$h_1(-65) = -0.00295 = -h_1(65)$	$h_1(-15) = -0.02107 = -h_1(15)$
$h_1(-63) = -0.00314 = -h_1(63)$	$h_1(-13) = -0.02444 = -h_1(13)$
$h_1(-61) = -0.00337 = -h_1(61)$	$h_1(-11) = -0.02901 = -h_1(11)$
$h_1(-59) = -0.00358 = -h_1(59)$	$h_1(-9) = -0.03557 = -h_1(9)$
$h_1(-57) = -0.00385 = -h_1(57)$	$h_1(-7) = -0.04560 = -h_1(7)$
$h_1(-55) = -0.00408 = -h_1(55)$	$h_1(-5) = -0.06380 = -h_1(5)$
$h_1(-53) = -0.00436 = -h_1(53)$	$h_1(-3) = -0.10099 = -h_1(3)$
$h_1(-51) = -0.00466 = -h_1(51)$	$h_1(-1) = -0.32064 = -h_1(1)$
$h_1(-49) = -0.00497 = -h_1(49)$	

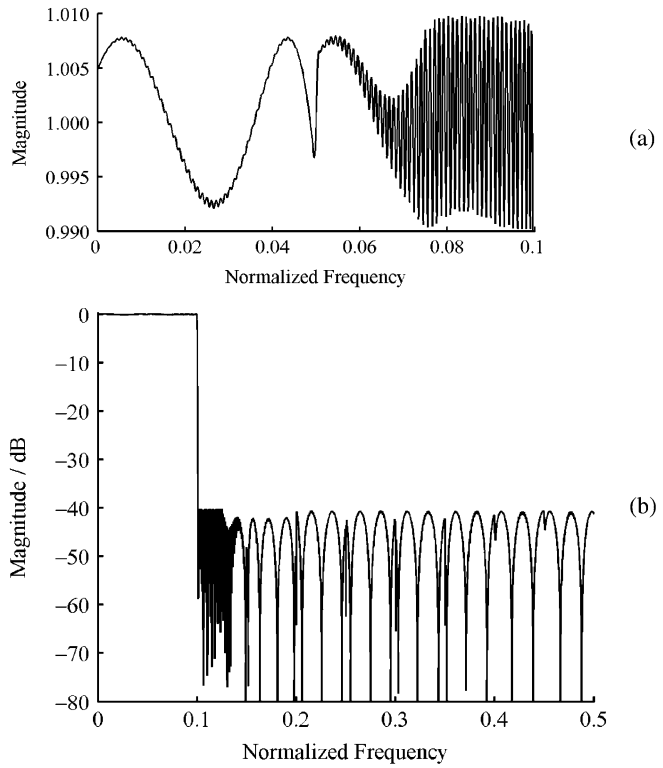

Fig. 9. Frequency response of a multirate filter. (a) Passband response. (b) Overall response.

Using the equations developed in [7] for the classical FRM technique, the values of M is 6 and the lengths of the bandedge-shaping and masking filters are 121, 62, and 62 respectively. Implementing the bandedge-shaping filter using the polyphase technique, the computational rate is $148.2 (= 62 + 62 + 121/5)$ multiplications per output sample.

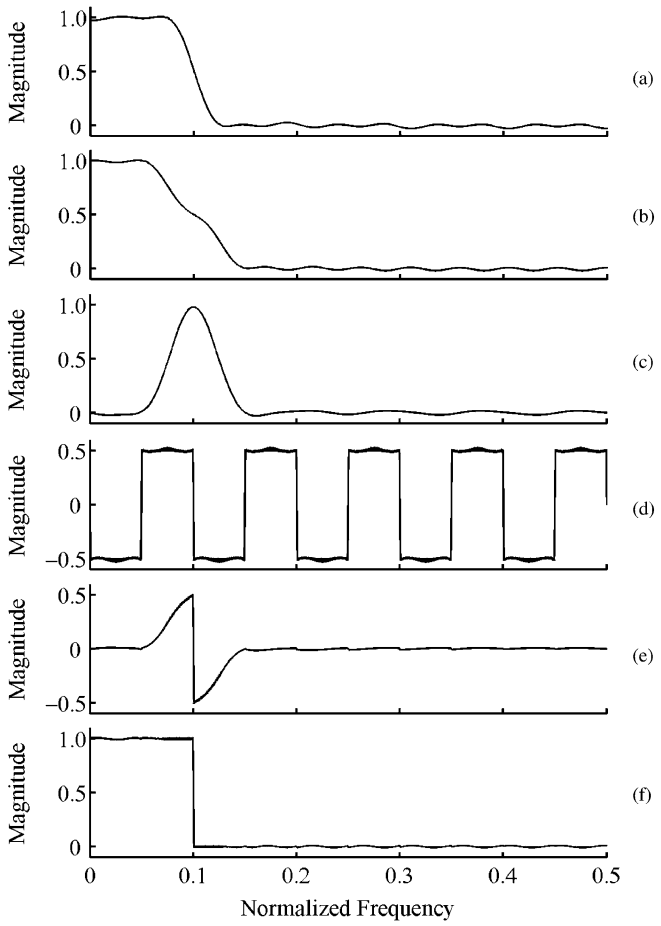

Fig. 10. Frequency responses of the subfilters. (a) $H_M(z)$, (b) $H_s(z)$, (c) $H_d(z)$, (d) $H_1(z^{10})$, (e) $H_1(z^{10})H_d(z)$, and (f) $H_s(z) + H_d(z)H_1(z^{10})$.

XI. VERY NARROWBAND FILTER FOR L EVEN

If the passband width of the filter is very narrow, the general structure of Fig. 1 degenerates into the IFIR [36] structure shown in Fig. 11. The frequency responses of the overall filter as well as those of its subfilters are shown in Fig. 12.

$$H(z) = H_a(z^M)H_{Ma}(z). \tag{53}$$

Consider the case where $H_a(z^M)$ is a halfband filter so that $H_a(z^M)$ can be written in the form of (8). Thus, we have

$$H(z) = H_1(z^M)H_{Ma}(z) + 0.5H_{Ma}(z). \tag{54}$$

The structure for implementing (54) is shown in Fig. 13. Note that $H_1(z^M)$ is a filter where consecutive taps are separated by $2M$ delays. Narrowband synthesis corresponds to the case where $2M$ is the smallest integer larger than or equal to L. Thus, $M = L/2$. The transition widths of $H_{Ma}(z)$ and $H_a(z)$ are $2\pi/M - (\omega_s + \omega_p)$ and $2\pi\beta M$, respectively. Note that $\omega_s + \omega_p = 2\pi/L$. The number of nonzero coefficients for $H_1(z)$ is given by (33), i.e., N_0/L since $M = L/2$. The number of coefficients

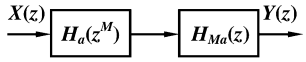

Fig. 11. FRM technique for the synthesis of narrowband filter.

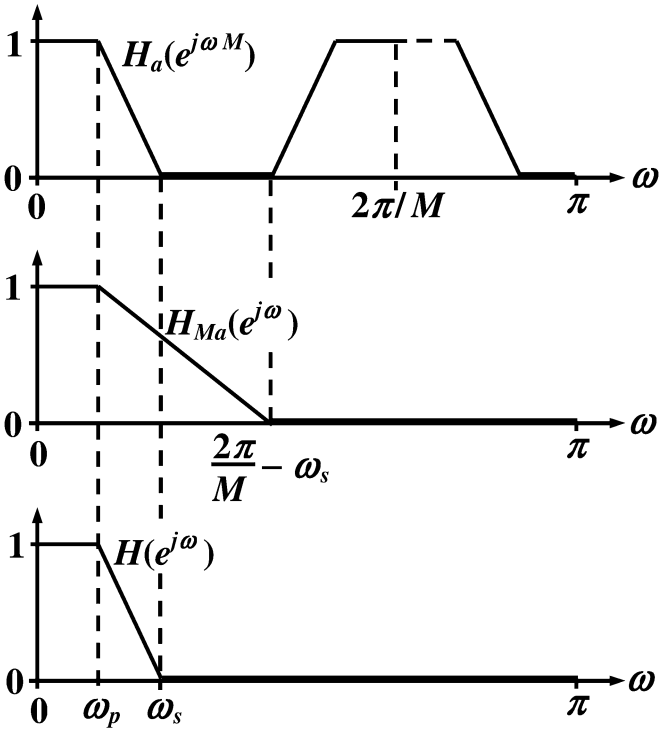

Fig. 12. Frequency responses of the filters in narrowband masking.

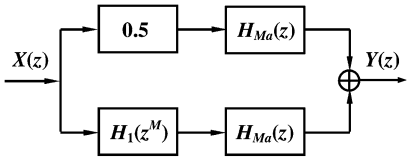

Fig. 13. Structure for implementing (54), where $M = L/2$.

for $H_{Ma}(z)$ is $\beta L N_0$. Thus, the frequency response masking technique will produce a saving if

$$N_0/L + 2\beta L N_0 < N_0 \tag{55a}$$

i.e., if

$$\beta < (L-1)/2L^2 \approx 1/(2L) \text{ for large } L. \tag{55b}$$

As already discussed in Section VIII, in polyphase implementation, exploitation of the coefficient symmetry of $H_{Ma}(z)$ to reduce computational complexity leads to other complications, but the symmetry of $H_1(z)$ can be exploited very easily. If the symmetry of $H_1(z)$ is exploited but not that of $H_{Ma}(z)$, the frequency response masking technique will produce a saving if

$$\beta < (2L-1)/4L^2 \approx 1/(2L) \text{ for large } L. \tag{55c}$$

XII. Conclusion

The FRM technique essentially produces a system of subfilters connected in cascade and in parallel. As a result, the computational complexity of a filter synthesized using the conventional FRM technique may not decrease as rapidly with increasing interpolation/decimation factor as it should be in multirate application. In this paper, we presented a novel variant of the FRM technique for interpolation or decimation. In this new variant, the computational complexity reduces as rapidly as the interpolation or decimation factor increases.

Appendix
[32]

$$N_0 \approx \frac{\Phi_1(\delta_p,\delta_s)}{\beta} + \Phi_2(\delta_p,\delta_s)\beta + 1$$

$$\Phi_1(\delta_p,\delta_s) = [a_1(\log_{10}\delta_1)^2 + a_2\log_{10}\delta_1 + a_3] \times \log_{10}\delta_2 + [a_4(\log_{10}\delta_1)^2 + a_5\log_{10}\delta_1 + a_6]$$

$$a_1 = 5.309 \times 10^{-3} \quad a_2 = 7.114 \times 10^{-2}$$

$$a_3 = -4.761 \times 10^{-1} \quad a_4 = -2.66 \times 10^{-3}$$

$$a_5 = -5.941 \times 10^{-1} \quad a_6 = -4.278 \times 10^{-1}$$

$$\Phi_2(\delta_p,\delta_s) = 11.012\,17 + 0.512\,44 \times (\log_{10}\delta_1 - \log_{10}\delta_2).$$

References

[1] R. E. Crochiere and L. R. Rabiner, *Multirate Digital Signal Processing*. Englewood Cliffs, NJ: Prentice-Hall, 1983.

[2] M. G. Bellanger, J. L. Daguet, and G. P. Lepagnol, "Interpolation, extrapolation, and reduction of computation speed in digiter filters," *IEEE Trans. Acoust., Speech, Signal Process.*, vol. ASSP-22, pp. 231–235, Aug. 1974.

[3] R. R. Shively, "On multistage finite impulse response (FIR) filters with decimation," *IEEE Trans. Acoust., Speech, Signal Process.*, vol. ASSP-23, pp. 353–357, Aug. 1975.

[4] T. Saramäki, "A class of linear-phase FIR filters for decimation, interpolation, and narrow-band filtering," *IEEE Trans. Acoust., Speech, Signal Process.*, vol. ASSP-32, pp. 1023–1036, Oct. 1984.

[5] H. Johansson and L. Wanhammar, "Filter structures composed of allpass and FIR filters for interpolation and decimation by a factor of two," *IEEE Trans. Circuits Syst. II: Analog Digit. Signal Process.*, vol. 46, pp. 896–905, Jul. 1999.

[6] Y. C. Lim, "Frequency-response masking approach for the synthesis of sharp linear phase digital filters," *IEEE Trans. Circuits Syst.*, vol. CAS-33, pp. 357–364, Apr. 1986.

[7] Y. C. Lim and Y. Lian, "The optimum design of one- and two-dimensional FIR filters using the frequency response masking technique," *IEEE Trans. Circuits Syst. II: Analog Digit. Signal Process.*, vol. 40, pp. 88–95, Feb. 1993.

[8] M. G. Bellanger, "Improved design of long FIR filters using the frequency masking technique," in *Proc. IEEE Int. Conf. Acoust. Speech. Signal Processing*, 1996, pp. 1272–1275.

[9] T. Saramäki, Y. C. Lim, and R. Yang, "The synthesis of half-band filter using frequency-response masking technique," *IEEE Trans. Circuits Syst. II: Analog Digit. Signal Process.*, vol. 42, pp. 58–60, Jan. 1995.

[10] G. Rajan, Y. Neuvo, and S. K. Mitra, "On the design of sharp cutoff wide-band FIR filters with reduced arithmetic complexity," *IEEE Trans. Circuits Syst.*, vol. 35, no. 11, pp. 1447–1454, Nov. 1988.

[11] H. Johansson and L. Wanhammar, "High-speed recursive digital filters based on the frequency-response masking approach," *IEEE Trans. Circuits Syst. II: Analog Digit. Signal Process.*, vol. 47, pp. 48–61, Jan. 2000.

[12] W. S. Lu and T. Hinamoto, "Optimal design of frequency-response-masking filters using semidefinite programming," *IEEE Trans. Circuits Syst. I: Fundam. Theory Appl.*, vol. 50, no. 4, pp. 557–568, Apr. 2003.

[13] ——, "Optimal design of IIR frequency-response-masking filters using second-order cone programming," *IEEE Trans. Circuits Syst. I: Funda Theory Appl.*, vol. 50, no. 11, pp. 1401–1412, Nov. 2003.

[14] M. B. Furtado, P. S. R. Diniz, and S. L. Netto, "Optimized prototype filter based on the FRM approach for cosine-modulated filter banks," *Circuits, Syst., Signal Process.*, vol. 22, no. 2, pp. 193–210, Mar./Apr. 2003.

[15] L. C. R. Barcellos, S. L. Netto, and P. S. R. Diniz, "Optimization of FRM filters using the WLS-Chebyshev approach," *Circuits, Syst., Signal Process.*, vol. 22, no. 2, pp. 99–113, Mar./Apr. 2003.
[16] O. Gustafsson, H. Johansson, and L. Wanhammar, "Single filter frequency masking high-speed recursive digital filters," *Circuits, Syst., Signal Process.*, vol. 22, no. 2, pp. 219–238, Mar./Apr. 2003.
[17] T. Saramaki and Y. C. Lim, "Use of the Remez algorithm for designing FRM based FIR filters," *Circuits, Syst., Signal Process.*, vol. 22, no. 2, pp. 77–97, Mar./Apr. 2003.
[18] H. Johansson and T. Saramaki, "Two-channel FIR filter banks utilizing the FRM approach," *Circuits, Syst., Signal Process.*, vol. 22, no. 2, pp. 157–192, Mar./Apr. 2003.
[19] Y. Lian and C. Z. Yang, "Complexity reduction by decoupling the masking filters from bandedge shaping filter in FRM technique," *Circuits, Syst., Signal Process.*, vol. 22, no. 2, pp. 115–135, Mar./Apr. 2003.
[20] Y. Lian, "Complexity reduction for FRM based FIR filters using the prefilter-equalizer technique," *Circuits, Syst., Signal Process.*, vol. 22, no. 2, pp. 137–155, Mar./Apr. 2003.
[21] Y. C. Lim, Y. J. Yu, H. Q. Zheng, and S. W. Foo, "FPGA Implementation of digital filters synthesized using the FRM technique," *Circuits, Syst., Signal Process.*, vol. 22, no. 2, pp. 211–218, Mar./Apr. 2003.
[22] T. Saramaki, J. Yli-Kaakinen, and H. Johansson, "Optimization of frequency-response-masking based FIR filters," *Circuits, Syst., Comput.*, vol. 12, no. 5, pp. 563–590, Oct. 2003.
[23] W. R. Lee, V. Rehbock, and K. L. Teo, "Frequency-response masking based FIR filter design with power-of-two coefficients and suboptimum PWR," *Circuits, Syst., Comput.*, vol. 12, no. 5, pp. 591–600, Oct. 2003.
[24] O. Gustafsson, H. Johansson, and L. Wanhammar, "Single filter frequency-response masking FIR filter," *Circuits, Syst., Comput.*, vol. 12, no. 5, pp. 601–630, Oct. 2003.
[25] S. L. Netto, L. C. R. de Barcellos, and P. S. R. Diniz, "Efficient design of narrowband cosine-modulated filter banks using a two-stage frequency-response masking approach," *Circuits, Syst., Comput.*, vol. 12, no. 5, pp. 631–642, Oct. 2003.
[26] Y. Lian, "A modified frequency response masking structure for high-speed FPGA implementation of programmable sharp FIR filters," *Circuits, Syst., Comput.*, vol. 12, no. 5, pp. 643–654, Oct. 2003.
[27] S. W. Foo and W. T. Lee, "Application of fast filter bank for transcription of polyphonic signals," *Circuits, Syst., Comput.*, vol. 12, no. 5, pp. 654–674, Oct. 2003.
[28] Y. C. Lim and R. Yang, "The synthesis of linear-phase multirate frequency-response-masking filters," in *Proc. IEEE Int. Symp. Circuits Systems*, 1997, pp. 2341–2344.
[29] H. Johansson, "A class of M th-band linear-phase FIR filters synthesized using the frequency-response-masking approach," in *Proc. IEEE Nordic Signal Process. Symp.*, Hurtigruten, Norway, 2002.
[30] ——, "Efficient FIR filter structures based on the frequency-response-masking approach for interpolation and decimation by a factor of two," in *Proc. 2nd Int. Workshop Spectral Methods Multirate Signal Process.*, Toulouse, France, 2002, pp. 73–76.
[31] ——, "Efficient frequency-response-masking based FIR filter structures for interpolation and decimation," in *Proc. 3rd Int. Workshop Spectral Methods Multirate Signal Processing*, Barcelona, Spain, 2003, pp. 59–62.
[32] O. Herrmann, L. R. Rabiner, and D. S. K. Chan, "Practical design rules for optimum finite impulse response lowpass digital filters," *Bell Syst. Tech. J.*, vol. 52, pp. 769–799, July–Aug. 1973.
[33] T. Saramäki and S. K. Mitra, "Multiple branch FIR filters for sampling rate conversion," in *Proc. IEEE Int. Conf. Circuit, Syst.*, 1992, pp. 1007–1010.
[34] S. K. Mitra, A. Mahalanobis, and T. Saramäki, "Generalized structural subband decomposition of FIR filters and its application in efficient FIR filter design and implementation," *IEEE Trans. Circuits Syst. II: Analog Digit. Signal Process.*, vol. 40, pp. 363–374, Jun. 1993.
[35] P. Arian, T. Saramäki, and S. K. Mitra, "A systematic technique for optimization multiple branch FIR filters for sampling rate conversion," in *Proc. IEEE Int. Conf. Circuit, Syst.*, vol. IV, 2002, pp. 1–4.
[36] Y. Neuvo, C.-Y. Dong, and S. K. Mitra, "Interpolated finite impulse response digital filters," *IEEE Trans. Acoust., Speech, Signal Process.*, vol. ASSP-32, pp. 563–570, Jun. 1984.

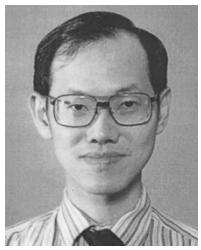

Yong Ching Lim (S'80–M'80–SM'92–F'00) received the A.C.G.I. and B.Sc. degrees in 1977 and the D.I.C. and Ph.D. degrees in 1980, all in electrical engineering, from Imperial College, University of London, London, U.K.

From 1980 to 1982, he was a National Research Council Research Associate with the Naval Postgraduate School, Monterey, CA. From 1982 to 2003, he was with the Department of Electrical Engineering, National University of Singapore. Since 2003, he has been with the School of Electrical and Electronic Enginerering, Nanyang Technological University, Singapore, where he is currently a Professor. His research interests include digital signal processing and VLSI circuits and systems design.

Dr. Lim received the 1996 IEEE Circuits and Systems Society's Guillemin-Cauer Award, the 1990 IREE (Australia) Norman Hayes Award, 1977 IEE (U.K.) Prize, and the 1974–1977 Siemens Memorial (Imperial College) Award. He served as a lecturer for the IEEE Circuits and Systems Society under the distinguished lecturer program from 2001 to 2002 and as an associate editor for the IEEE TRANSACTIONS ON CIRCUITS AND SYSTEMS from 1991 to 1993 and from 1999 to 2001. He also served as an Associate Editor for *Circuits, Systems, and Signal Processing* from 1993 to 2000. He served as the Chairman of the DSP Technical Committee of the IEEE Circuits and Systems Society from 1998 to 2000. He served in the Technical Program Committee's DSP Track as the Chairman of ISCAS'97 and ISCAS'00 and as a Co-chairman of ISCAS'99. He is a member of Eta Kappa Nu.

Rui Yang received the B.S. degree in electrical engineering in 1992 from Peking University, Beijing, China. She joined the DSP and VLSI Laboratory of the National University of Singapore in 1993, from which she received the Ph.D. degree in electrical engineering in 1997.

Her research interests has been in the area of the design and synthesis of very sharp FIR filters with very low computational complexity and implementation cost. She joined Hal Computer Systems, a subsidiary of Fujitsu, in 1998, involving herself with R&D projects for server area networks. She is currently a Senior Design Engineer with Agilent Technology Inc., Milpitas, CA. Her interests include micro-architecture, design, and verification for storage area network ASICs.